Reprinted from

AGRICULTURAL AND FOREST METEOROLOGY

An International Journal

Radiative transfer in shrub savanna sites in Niger: preliminary results from HAPEX-Sahel. 3. Optical dynamics and vegetation index sensitivity to biomass and plant cover

W.J.D. van Leeuwen[*,a], A.R. Huete[a], J. Duncan[b], J. Franklin[b]

[a]*Department of Soil and Water Science, University of Arizona, Tucson, AZ 85721, USA*
[b]*Department of Geography, San Diego State University, San Diego, CA 92182, USA*

ELSEVIER

AGRICULTURAL AND FOREST METEOROLOGY

Scope of the journal

Agricultural and Forest Meteorology is an international journal for the publication of articles and reviews in the interdisciplinary fields of meteorology and plant, animal and soil sciences as applied to heat, mass and momentum transfer in agriculture, forestry or natural ecosystems. Articles must appeal to an international audience. Emphasis is on basic and applied scientific research to problems in agriculture, forestry and natural ecosystems. Theoretical models should always be tested against experimental data. Typical topics include radiation transfer in plant canopies, evapotranspiration, energy transfer, air turbulence in and above plant canopies, forest-fire/weather interactions, pollutant fluxes to vegetation in the field and enclosures, trace gas fluxes in man-made and natural ecosystems, climatology of plant distributions, glasshouse energy balances and climatology, animal biometeorology. Special issues devoted to single topics, conference proceedings and comprehensive reviews are also published.

Radiative transfer in shrub savanna sites in Niger: preliminary results from HAPEX-Sahel. 3. Optical dynamics and vegetation index sensitivity to biomass and plant cover

W.J.D. van Leeuwen[*,a], A.R. Huete[a], J. Duncan[b], J. Franklin[b]

[a]Department of Soil and Water Science, University of Arizona, Tucson, AZ 85721, USA
[b]Department of Geography, San Diego State University, San Diego, CA 92182, USA

Abstract

A shrub savannah landscape in Niger was optically characterized utilizing blue, green, red and near-infrared wavelengths. Selected vegetation indices were evaluated for their performance and sensitivity to describe the complex Sahelian soil/vegetation canopies. Bidirectional reflectance factors (BRF) of plants and soils were measured at several view angles, and used as input to various vegetation indices. Both soil and vegetation targets had strong anisotropic reflectance properties, rendering all vegetation index (VI) responses to be a direct function of sun and view geometry. Soil background influences were shown to alter the response of most vegetation indices. N-space greenness had the smallest dynamic range in VI response, but the n-space brightness index provided additional useful information. The global environmental monitoring index (GEMI) showed a large VI dynamic range for bare soils, which was undesirable for a vegetation index. The view angle response of the normalized difference vegetation index (NDVI), atmosphere resistant vegetation index (ARVI) and soil atmosphere resistant vegetation index (SARVI) were asymmetric about nadir for multiple view angles, and were, except for the SARVI, altered seriously by soil moisture and/or soil brightness effects. The soil adjusted vegetation index (SAVI) was least affected by surface soil moisture and was symmetric about nadir for grass vegetation covers. Overall the SAVI, SARVI and the n-space vegetation index performed best under all adverse conditions and were recommended to monitor vegetation growth in the sparsely vegetated Sahelian zone.

* Corrresponding author.

1. Introduction

Remote sensing data can be used to monitor seasonal vegetation growth at different scales and temporal frequencies. By making use of vegetation and soil specific optical properties, vegetation indices (VIs) are developed to study a wide variety of biomes. Spectral vegetation indices are used to estimate percentage green cover, biomass, leaf area index (LAI) and photosynthetic activity (Colwell, 1974; Baret and Guyot, 1991). From this knowledge, information can be inferred as to which environmental factors, e.g. climate, are governing a particular landscape. Also, the biophysical and bio-geochemical properties as well as anthropogenic influences are manifested by each individual biome and are the boundary conditions for its development. These biomes are used as indicators of climatic and global changes at the earth's surface inferred by mass and energy balance disturbance. More specifically, global circulation models (GCMs) use remotely sensed land cover products to predict climate and global change. In particular, the spatial and temporal information from vegetation index products can be used in energy and water balance models as parameters governing evapotranspiration (Jackson et al., 1987; Moran et al., 1989).

Optical remote sensing data of land surfaces in semi-arid, subtropical environments are often difficult to interpret because neither bare soil nor vegetation are dominant in the landscape. The diversity of soil, vegetation and other components at the earth's surface contribute to the spectral response and form complex spectral mixtures. The spectral signatures, therefore, are determined by the radiative interaction of the components themselves, as well as by the atmosphere and the sun and sensor positions. The interpretation of remote sensing data will be improved if the controlling parameters affecting vegetation indices are properly modeled. Furthermore the ground, biophysical sampling procedure of remote sensing experiments in the sparsely vegetated Sahelian region needs special attention because of seasonality and the spatial distribution of vegetation.

One of the problems in modeling the water and energy balance over desert areas is the heterogeneous distribution of vegetation. Generally, the natural vegetation is sparse and has a clumped spatial pattern. With high spatial resolution measurements it would be possible to derive the ratio of vegetated and non-vegetated areas, providing an important parameter in water and energy balance models, and erosion models. Since the impact of wind and water erosion is partly governed by the vegetation cover and its spatial distribution, a parameter describing vegetation spatial pattern would give an indication of potential erosion. Also, the initial state of degradation (crusted soil surface) of the landscape is observed to be an important factor for seasonal vegetation growth. Seasonal dynamics of the Sahelian zone are mainly determined by the amount of rainfall and its spatial and temporal distribution (Justice et al., 1991; Wylie et al., 1991). Townshend and Justice (1986) showed that African vegetation dynamics can be monitored using temporally composited NDVI (normalized difference vegetation index) images of AVHRR (advanced very high resolution radiometer) on a global scale.

Presently, improved vegetation indices are being developed to monitor terrestrial vegetation from space platforms. Most vegetation indices are computed from the

difference between the reflectance factors in the near infrared (ρ_{NIR}) and the red (ρ_{red}) wavelengths. The normalized difference vegetation index

$$NDVI = (\rho_{NIR} - \rho_{red})/(\rho_{NIR} + \rho_{red}) \qquad (1)$$

has been used extensively over the last 15 years with successful results, but has also been found to be sensitive to soil background, atmosphere and sun and view geometry. The soil adjusted vegetation index

$$SAVI = (1 + L)(\rho_{NIR} - \rho_{red})/(\rho_{NIR} + \rho_{red} + L) \qquad (2)$$

is a modified version of the NDVI whereby a correction factor (L) is introduced to minimize secondary backscattering of canopy transmitted-soil reflected radiation (Huete, 1988; $L = 0.5$), thus normalizing the soil background effect and allowing for a partial correction of view angle effects (Huete et al., 1992). The global environmental monitoring index (Pinty and Verstraete, 1992)

$$GEMI = \gamma(1 - 0.25\gamma) - ((\rho_{red} - 0.125)/(1 - \rho_{red})) \qquad (3)$$

where

$$\gamma = (2(\rho_{NIR}^2 - \rho_{red}^2) + 1.5\rho_{NIR} + 0.5\rho_{red})/(\rho_{NIR} + \rho_{red} + 0.5)$$

was designed to reduce the effects of unwanted atmospheric perturbations of AVHRR data, without losing its sensitivity to the vegetation cover.

The atmosphere resistant vegetation index and soil atmosphere resistant vegetation index (Kaufman and Tanré, 1992),

$$ARVI = (\rho_{NIR} - 2\rho_{red} + \rho_{blue})/(\rho_{NIR} + 2\rho_{red} - \rho_{blue}) \qquad (4)$$

$$SARVI = (1 + L)(\rho_{NIR} - 2\rho_{red} + \rho_{blue})/(\rho_{NIR} + 2\rho_{red} - \rho_{blue} + L) \qquad (5)$$

incorporate the reflectance factor of the blue channel (ρ_{blue}) to correct for atmospheric aerosols on the red channel. Although ARVI and SARVI correct for atmospheric aerosol effects, it must be noted that the spectral bands have to be corrected for Rayleigh and ozone scattering and absorption effects before ARVI and SARVI are computed. These self atmosphere-correcting indices perform best for well-vegetated areas with performance levels dropping for bare soils (Kaufman and Tanré, 1992). Both ARVI and SARVI were developed with simulated MODIS (moderate resolution imaging spectrometer) bands, but Kaufman and Tanré (1992) stated these indices can be used for Landsat thematic mapper bands as well.

The n-space indices (Jackson, 1983), like the perpendicular vegetation index (PVI; Richardson and Wiegand, 1977) and the four-dimensional greenness vegetation index (GVI; Kauth and Thomas, 1976; Huete et al., 1984), have physical significance in not only discriminating vegetation but also providing information from the soil background. In this study, the seasonal-optical dynamics of different soil and vegetation types will be characterized and evaluated with respect to view and sun geometry, soil background influences, dynamic range and vegetation growth.

This preliminary research was conducted in preparation for the 1992 Hydrologic and Atmospheric Pilot Experiment (HAPEX) in the Sahel (Goutorbe et al., 1994).

One of the objectives of the HAPEX-Sahel project was to investigate the utility of remote sensing inversion algorithms in the Sahelian region of West Africa. Ground based observations and information are necessary to validate the satellite inversion algorithms. The purpose of this paper was to perform a ground-based evaluation on recently developed VIs, utilizing the ground data set collected in a savannah landscape in Niger, in order to determine which are most appropriate for vegetation analysis in the Sahelian zone. Of interest to this study was exploring the extent of anisotropic reflectance behavior of grassland canopies in order to determine what BRF (bidirectional reflectance factor) measurements are necessary to implement an effective vegetation monitoring index. Since both ARVI and SARVI are claimed to be sensitive to vegetation cover (with the SARVI correcting for soil background), they were evaluated in comparison to NDVI, SAVI and PVI. We recognize that ARVI and SARVI normalize variations in atmospheric aerosol concentrations, but we are testing if the blue band inclusion is aggravating the soil problem. Furthermore, we hypothesize that a ground data-set that is nearly unaffected by atmosphere, should behave similarly to a minimal, aerosol-affected data set. Thus, we can examine the ARVI and SARVI performances over these variations in aerosol contents. Although the GEMI was developed to correct atmospheric contaminated AVHRR data, the response of this index to non-atmospheric affected data was also examined. This paper is the third in a series of three studies of radiative transfer and primary production in shrub savanna sites in Niger (Franklin et al., 1994; Bégué et al., 1994).

1.1. Description of Niger study sites

The area selected for this study is part of the larger HAPEX-Sahel site which is located between 2°–3°E and 13°–14.5°N. Elevation differences of the complete site (mean elevation ≈ 240 m above sea-level) are within 100 m. Several typical Sahelian landscapes were chosen in a region west of the town of Ouallam (Latitude 14.3°N, Longitude 2°E), about 100 km north of Niamey, based on a visual satellite image stratification and ground survey.

The region was stratified into five land units: (1) fallow bush/grassland; (2) semi-desert grassland; (3) millet (*Pennisetum* spp.) fields; (4) degraded bushland; (5) tiger-bush plateau. This stratification is related to the general toposequence of this region. The first three land units are present in the relatively flat and lower elevation, wide, sandy valleys. The degraded bushland areas are found on the slopes between the valleys and the plateaus. Degraded bushland is also present in the valleys as a result of erosion and anthropogenic activity. The tigerbush patterns on the higher elevated plateaus are scarce, especially in comparison with the southern part of the HAPEX study area.

The concentrations of herbaceous and woody species are related to the local site conditions (Justice and Hiernaux, 1986). Post-storm rainfall distribution and infiltration largely determine the distribution of vegetation cover, density and species. *Aristida* spp. were the dominating grasses at the fallow grass/bushland, but *Eragrostis tremula* and *Cenchrus bifloris* were also common. The fallow grass/ bushland hosted many forbs among which were *Mitracarpus scaber*, *Alysicarpus*
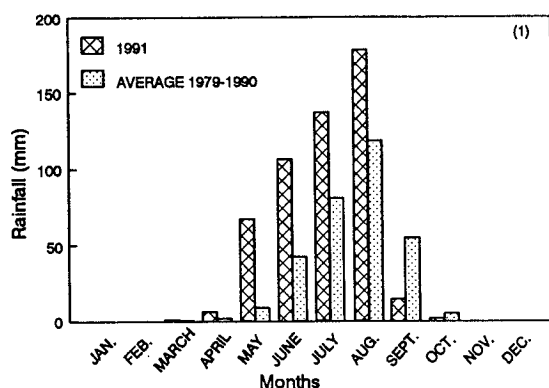
Fig. 1. Monthly rainfall distribution for Ouallam, 15 km east of study sites. Comparison of 1991 rainfall with average of 12 years (source: INRAN, Ouallam).

ovalifolius, Cassia mimosoïdes, Sida spp. and *Gisekia pharnacioïdes*. The degraded bushland was dominated by *Cenchrus bifloris*, intermixed with the forbs *Mitracarpus scaber* and *Cassia mimosoïdes. Guiera senegalensis* is the dominant shrub in this region and occasionally *Combretum micranthum* and *Combretum gluttinosum* are found.

Vegetation growth in this region is generally limited by the seasonal rainfall. The 1991 rainfall started early and was fairly well-distributed over the growing season. The cumulative precipitation reached about 510 mm, which is 200 mm above average. Monthly rainfall is presented in Fig. 1 (source: INRAN, Institut National de Recherches Agronomiques du Niger, Ouallam, unpublished data, 1991). Because water availability was sufficient, soil nutrient deficiencies were more of a factor in limiting primary production (Payne et al., 1990). Millet fields where fertilizers were applied were observed to have higher production than non-fertilized parcels (personal observation). The intense monsoon rains caused severe sheet and gully erosion. The loamy sand soils lose their topsoil to water erosion when increased run-off occurs, caused by surface crust formation and lack of vegetation cover. Wind erosion occurs during the dry season when the Harmattan winds deposit and transport soil particles causing dune formations. Furthermore, the pressure on the grassland and bushland is increased through fuel wood collection and grazing practices. Large herds of goats and sheep were observed almost daily visiting parts of the grass/bushland study area. The goats had a special preference for the leaves of *Guiera senegalensis* as opposed to the grasses. All of the above factors contributed to the marked spatial heterogeneity of both the plant cover and soils.

2. Methods and instrumentation

2.1. BRF of soil and vegetation targets

Reflectance data were collected with an Exotech radiometer (Exotech International, Gaithesburg, MD, USA) with 15° field of view (FOV) lenses. The four wave-

bands included Landsat TM1 (0.45–0.52 μm) and SPOT XS1 (0.50–0.59 μm), XS2 (0.61–0.69 μm) and XS3 (0.79–0.90 μm) bands. The radiometer was mounted on a lightweight BRF apparatus to measure bidirectional reflectances over the target of interest at the bush/grassland and the degraded bushland sites, using various view angles, mostly along the principal plane of the sun. The BRF apparatus allowed for multiple view measurements of the same surface target and was similar to that described in Jackson et al. (1990). View angles were calibrated in the field and varied from −50° to +50° with increments of approximately 6°. At nadir view angles, the instrument, set at 15° FOV, was mounted 2.70 m above the surface forming a target pixel of about 70 cm in diameter. For each view angle, the same target was measured twice. A horizontal BaSO$_4$ reference panel, which was calibrated for non-lambertian properties, was measured from a nadir view angle immediately before and after the set of measurements. The BRF was calculated by dividing the reflected radiance response for each view angle by the reflected irradiance as measured from the horizontal reference panel. The time lapse for the whole measurement sequence was about 4 min.

Measurements were made during the growing season in the morning and the afternoon for different view zenith and azimuth angles, solar zenith angles, vegetation covers, and soils, if clouds were not obscuring the sun. Most of the BRF data presented were collected at a nominal solar zenith angle of 40° in the principal plane of the sun, if not stated differently. Some irregularities in the data can occur when the antisolar view angle is approximately the same as the solar zenith angle (hot spot). At this view angle the radiometer was partially shading the target causing a lower reflectance response.

An overview of the data collected and used in the analysis is presented in Table 1. On DOY (day of year) 213, bidirectional reflectance measurements were made over a target with approximately 50% green grass cover (Table 1). Later in the growing season (DOY 221), bidirectional reflectance measurements were made at the degraded bushland site of a mixed grass/forb vegetation target (40% cover), and three different non-vegetated targets with slightly moist soils (wet soil surface was evident). The sandy soil in the degraded bushland resembled the sandy soil at the fallow grassland. In addition to being optically characterized with the Exotech radiometer for different view and sun geometries, Munsell color was also determined to give an indication of the brightness of the soils (Table 2). On DOY 226, bidirectional measurements were made over *Cassia mimosoïdes* which has planophile leaves and was completely covering the soil (100% cover). On DOY 233, diurnal bidirectional measurements were made over canopies of 20 and 80% vegetation covers, mostly consisting of erectophile grasses.

2.2. Radiometric measurements of components and landscapes

Soil and vegetation components representative of the different landscapes, were radiometrically sampled in their natural environment to obtain 'pure' spectral signatures. The radiometer was pointed at nadir over homogeneous soil and vegetation targets and ten measurements were averaged. After each measurement the radiometer was slightly moved to obtain a representative sample.

Table 1
Overview and conditions of radiometric and biophysical data collection

DOY	Green cover	Target	View azimuth angle	Solar zenith angle	Surface soil moisture	Dry green biomass (kg ha^{-1})
BRF data			PP, OP, TP[b]			
213	50%	grass[a]	79°, 169°, 124°	46°, 43°, 39°	moist	—
213	50%	grass	259°	30° (p.m.)	dry and wet	—
221	40%	grass/forb	82°	46°	moist	—
226	100%	Cassia	85°	39°	dry	3656
233	20%	grass[a]	89°	36°	wet	743
233	80%	grass[a]	89°	37°	wet	3812
221	0%	soils	82°	44°, 41°, 40°	moist	0
226	0%	sand & litter	84°	42°, 48° (p.m.)	dry	0
Nadir transect data						
206	17%	millet	—	37°	moist	—
206	40%	bush/grassland	—	41°	moist	814
211	40%	bush/grassland	—	41°	dry	814
227	41%	bush/grassland	—	42°	dry	1181
237	45%	bush/grassland	—	42°	moist	1684
210	18%	degraded bushland	—	39°	dry	—
227	21%	degraded bushland	—	31°	dry	—
237	22%	degraded bushland	—	32°	moist	—
243	< 1%	plateau	—	40°	dry	—

[a] Diurnal measurements were made for these targets.
[b] PP — solar principal plane; OP — orthogonal plane (90° with PP); TP — tertiary plane (45° with PP).

To examine temporal vegetation dynamics, bi-weekly radiometric transect measurements were made in the fallow grassland and degraded bushland sites (Table 1). Spectral reflectances were measured every 5 m along two parallel 1000 m transects. The parallel transects involved two operators walking approximately 75 m apart with a yoke and Exotech radiometer mounted at a height of approximately 1.90 m (target diameter is 45 cm). The transect at the fallow grassland was measured consistently at 09:00 h GMT under clear mornings to maintain the same solar zenith angle of about 40°. The transect at the degraded bushland was measured around 09:30 h GMT. On DOY 206, a 500 m transect through a millet field adjacent to the fallow grassland was radiometrically sampled every 2 m (Table 1). After this date the height of the millet plants exceeded the height of the radiometer mounted

Table 2
Munsell colors (hue-YR, value and chroma) of optically characterized soils

	Dry soil color	Wet soil color
Sandy soil	7.5Y/R 7/8	5 Y/R 5/8
Loamy sandy crust soil	5 Y/R 4/4	2.5 Y/R 3/6
Sandy lateritic gravel soil	7.5 Y/R 6/6	5 Y/R 3/6

on the yoke. A 1000 m transect on a lateritic plateau was measured on DOY 243 (Table 1).

Immediately before and after the transect or component radiance measurements, irradiance measurements over a calibrated $BaSO_4$ reference panel were made. The reflectance factors were calculated by ratioing the target response and the interpolated response of the plate at the time of the actual transect or component readings.

2.3. Transect percentage cover and biomass estimation

Herbaceous biomass samples were collected three separate times during the 5 week period. For each measurement period, ten samples of the herbaceous layer were clipped along one of the 1000 m transects using a 40 cm × 40 cm quadrangle. Shrubs and patches of bare soil were not sampled. The leaves were not stripped from the shrubs to avoid impact on the site and because many of the shrubs were leafless owing to browsing of goats. Since both shrubs ($\approx$ 4–9% cover) and patches of bare soil ($\approx$ 15–20% cover) were not dominant, we slightly underestimated the biomass by not sampling the shrubs and overestimated biomass by not sampling the bare soil areas. For all harvested samples green and senescent yellow biomass were separated and dried in an oven for 48 h at 80°C. Dry green biomass samples were then converted to standing crop per hectare (kg ha^{-1}) (Table 1).

Vegetation cover measurements were also made over all transects, using a step-point method (Bonham, 1989). A small point at the toe was marked and at every fourth step an observation of the ground cover was recorded. Beside the feature directly under this point, the feature directly above this point was recorded as well (Table 3) in order to get an indication of species composition. An estimate of cover of each feature is given in Table 3 for the fallow grassland and degraded bushland transects where biomass samples were collected as well.

Table 3

Percentage cover estimate for vegetation species and soil for fallow grassland and degraded bushland, at different times during the growing season

Component	Fallow bush/grassland			Degraded bushland		
	DOY 207	DOY 228	DOY 237	DOY 208	DOY 228	DOY 236
Bare soil	47.1	46.9	40.6	79.7	78.5	78.2
Litter	10.0	7.3	9.8	1.3	0.8	0.7
Green grass	32.2	37.5	42.6	4.8	6.3	4.8
Forbs	1.7	1.7	1.9	2.5	3.6	8.0
Guiera spp. (shrub)	9.0	4.9	3.9	10.4	10.0	8.3
C. Micranthum (shrub)	0	1.4	0.8	0.7	0.4	0
C. Glutinosum (shrub)	0	0.3	0.4	0.3	0	0
Other shrubs	0	0	0	0.3	0.4	0
Total green cover	42.9	45.8	49.6	19.0	20.7	21.1

3. Results and discussion

3.1. Spectral reflectances for soil, vegetation and landscapes

Pure component spectral signatures for representative soil and vegetation species are presented in Figs. 2(A) and 2(B), except for the grass cover which was never dense enough to form a pure component. The spectral reflectances for the soils gradually increased with wavelength. The amplitude of the signature is an indication of brightness, white sand being the brightest soil and the coarse lateritic gravel the darkest surface. For this region the darker soils were generally found at the degraded bushland and plateaus and the brighter soils in the bush/grassland and millet fields except for certain dark areas with accumulation of organic matter. The characteristic spectral reflectances for photosynthetic active vegetation was low in the red waveband owing to chlorophyll absorption and highly reflective in the NIR waveband owing to leaf cell structure (Fig. 2(B)). The spectral signature for non-photosynthetic litter was noticeably flat. The older leaves of the *Guiera senegalensis* appeared less pigmented (light green) and less lush in comparison with the younger leaves, and therefore had a higher reflectance in the red and lower in the NIR wavebands.

A combination of all these signatures (Figs. 2(A) and 2(B)) made up the overall signatures encountered over the major Sahelian landscape units (Fig. 2(C)), since these were mixtures of the different soils and vegetation species distributed across the different landscapes. The spectral signatures of the different landscapes, which were averages of the radiometric transects, (Fig. 2(C)) had an almost linear response with wavelength, except the plateau site, which had a spectral signature that closely resembled the sandy lateritic gravel spectral signature in Fig. 2(A). The spectral signature of the fallow grass/bushland site is observed to be brighter for a dry soil background than for a wet soil background (Fig. 2(C)). The 'landscape' spectral signatures more closely resembled the litter and bare soil signatures than those of the 'pure' vegetation, demonstrating the sparse nature of vegetation in the Sahel. Interestingly, the millet field (17% green cover and 75 cm high) and the fallow site (38% green grass cover) had nearly identical spectral signatures at this time of the year (end of July). The degraded bushland was much brighter than the densely vegetated areas.

Knowledge about the pure component spectral signatures aids in the analysis and inverse modeling of remotely sensed data. It can be used as a reference for the interpretation and utilization of data, especially with additional biophysical data. Representative 'pure' signatures of the leaves of *Guiera senegalensis* and millet can be used as a reference for 100% photosynthetic active vegetation. In order to calculate the 2-space and 4-space indices (PVI and GVI), pure spectral reflectances from dark and bright soils are needed. For a four-space index the reflectance of a pure green plant is also needed and an extra feature like a senescent vegetation component can be used to ascertain other features of the landscape.

3.2. View angle effects on reflectances

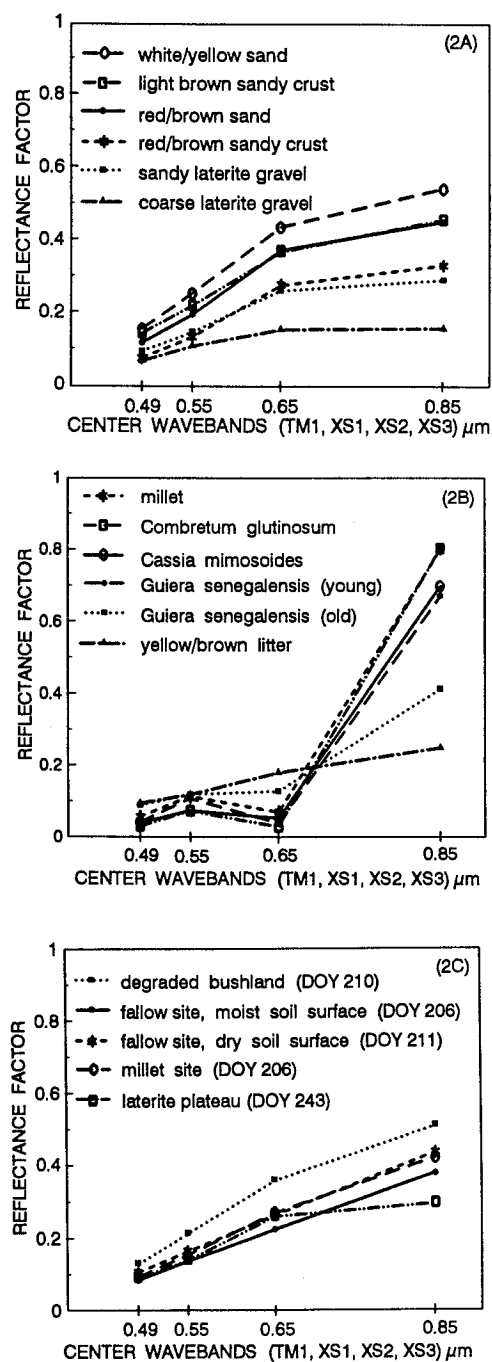For a more complete understanding of the 'mixed' optical characteristics of the

Fig. 2. Reflectance spectral signatures for different soil surfaces (A), and vegetation species (B). (C) shows a transect average spectral signature of stratified landscapes.

Sahelian landscapes, BRF optical measurements of vegetation and soils were made. Satellite sensors such as the AVHRR and SPOT often use multiple view angles to monitor the earth. If a sensor views a grassland (50% green cover) at nadir with plants of 40 cm height it will see a lot of soil (50%), however, when looking off nadir from an angle of 40°, it will see almost all grass. Thus, off-nadir view angles in this case alter the spectral information since the reflectances of different vegetation and soil targets are anisotropic with changing view angle. If the effects of view angle on the reflected radiation are known, it is possible to correct for these and more accurately interpret satellite imagery.

The BRFs of the four wavebands over eight targets are shown as a function of view angle in Figs. 3(A) and 3(B). Generally, reflectances in the antisolar view direction were up to 50% higher than those at nadir for all bands and for both vegetation and soil targets. The blue, green and red band continued to decrease from nadir to larger forward scatter view angles for green vegetation targets and for the soils, except the bright sand. The NIR waveband had an asymmetric concave response with view angle
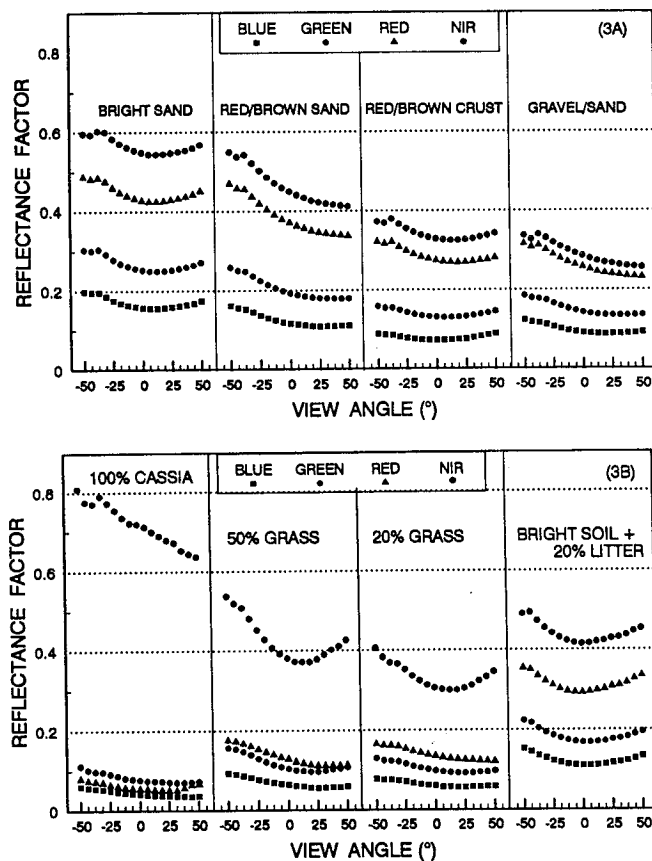

Fig. 3. View angle effect on the reflectances of major soil types (A; DOY 221 and 226), and different vegetation covers (B; DOY 233, 221 and 213), for TM1 (blue), XS1 (green), XS2 (red), and XS3 (NIR).

(minimum about nadir) for the green vegetated targets, but with *Cassia mimosoïdes* the NIR waveband continued to decrease in the forward scatter direction as well. This might be due to the fact that the *Cassia* was 100% green and could be considered a planophile plant (horizontal leaf angle distribution), while the grass targets were sparser and more erectophile (vertical leaf/stem angle distribution).

The vegetated targets reflected more in the antisolar direction because all plant components were illuminated by direct solar radiation. In the forward scatter direction the shaded components only reflected diffuse radiation, thus reducing the amount of total (direct and diffuse) reflected solar radiation. Owing to multiple backscattering inside a canopy and specular reflection, the NIR waveband also increased with larger view zenith angles in the forward scatter direction for some of the vegetation cover/soil combinations. Such a pattern should render the vegetation index response to be anisotropic. Because the crusted soil and bright sand surface had very little 'roughness', there was less anisotropy caused by forward direction shadowing by the roughness facets.

3.3. Vegetation index dynamics and effect of soil background

The selected VIs were evaluated with respect to their sensitivity to different vegetation covers, and the effect of view zenith angle and soil background. The results are presented in Table 4. The main criterion to determine whether the VIs were sensitive to green vegetation cover was by examining how well it separated different vegetation covers. For example, Figs. 4(A), 4(D) and 4(E) show that the NDVI, ARVI and SARVI could not separate the 40% green vegetation cover from a 20% green vegetation cover. The brightness index (Fig. 4(G)) shows that the 20% vegetation cover is a dark target compared with the 40 and 50% vegetation covers. Since the

Table 4
Evaluation of vegetation indices with respect to vegetation cover, soil background, view zenith angle and soil moisture

	Green vegetation sensitivity	Range of VIs	%VEN$_{soils}$[a] (nadir)	Response to view angle	%VEN$_{wetness}$[b] (nadir)
NDVI	medium	0–0.9	16.2	asymmetric	6.4
SAVI	good	0–0.8	16.3	symmetric	−0.3
ARVI	medium	−0.2–0.9	13.3	asymmetric	6.8
SARVI	medium/good	−0.2–0.8	12.0	asymmetric	1.8
GEMI	medium/good	0.1–1.1	31.3	fairly symm.	−2.1
2-space					
PVI	good	0–0.5	12.4	fairly symm.	−1.2
Brightness	bad	0.3–0.7	—	asymmetric	−13.3
4-space					
GVI	good	0–0.5	13.2	fairly symm.	−2.3
Brightness	bad	0.3–0.8	—	asymmetric	−13.3
Yellowness	bad	−0.1–0	—	asymmetric	−8.0

[a] For non-vegetated surfaces.
[b] VI response to surface soil moisture calculated for 50% green grass cover.

20% vegetation cover (wet soil background) had a lower brightness than the 40% vegetation cover (moist soil background), the NDVI, ARVI and SARVI (Fig. 4) could not distinguish these vegetation covers. The SAVI, PVI and GEMI (Fig. 4) were less affected by soil brightness and separated the 20% vegetation cover from the 40% vegetation cover. The response of VIs to soil moisture is a soil brightness effect that is minimized by some VIs. The range (bare soil to full cover; Table 4) gave an indication of the range of green vegetation sensitivity for different vegetation covers and species.

The three non-vegetated soils also varied in VI response. This represented a 'noise' factor in the assessment of sparse vegetation covers with VIs. Most soils at the sites were comparable with the bright sandy soil, which had a higher VI response than the darker soils. The dark lateritic gravel/sand surfaces on the plateaus had the lowest VI response, except with the GEMI where the opposite response was observed. The GEMI also had the widest response range to the three selected soils, approximately 0–0.4 (Fig. 4(F)). The larger the range of VI response to varying soil backgrounds, the lower the VI sensitivity to green vegetation. Litter gave a deceptive green vegetation response since it always increased the VI response relative to bare soils.

A quantitative method to determine the sensitivity of VIs to soil-vegetation mixtures was to examine the range of VI values from non-vegetated surfaces (bare soil, litter, etc.) relative to the VI dynamic range (soil to full cover). This results in a sensitivity measure of the lower limit of green vegetation detection, where

$$\%\text{VEN}_{soils} = 100(\text{VI}_{max} - \text{VI}_{min})_{soils}/(\text{VI}_{full\,canopy} - \text{VI}_{soils,\,mean}) \tag{6}$$

VEN_{soils} is the vegetation equivalent noise induced by non-vegetated surfaces. The absolute range in VI response, $\text{VI}_{max} - \text{VI}_{min}$, determined the 'soil noise' while subtraction of the mean of the bare soils ($\text{VI}_{soils,\,mean}$) from the VI response of a full canopy target ($\text{VI}_{full\,canopy}$) defined VI specific dynamic range. The $\text{VI}_{soils,\,mean}$ was considered the 'soil baseline' of each VI.

The percentage vegetation equivalent noise (VEN_{soils}) is a measure of the uncertainty in a VI for confidently discriminating bare soil from sparsely vegetated surfaces. Figure 5 shows resulting noise assessment for the different VIs at different view angles using a representative range of bare soils and a full canopy of *Cassia*. The percentage vegetation equivalent noise was lower in the forward direction (shaded side) than the antisolar view direction. The GEMI had the highest uncertainty (≈ 29–42%) and thus the worst vegetation signal response for bare soils. NDVI and SAVI had lower limits of uncertainty between approximately 15 and 20%, while ARVI, SARVI and PVI had uncertainties between approximately 8 and 16%. Thus, one could not reliably discriminate bare soil from a 30–40% green cover with the GEMI because both targets possess the same VI response. This uncertainty reduced to 10–20% with all other VIs (see Table 4).

The soil noise uncertainty can be reduced with prior knowledge of the soils within each landscape unit, thus reducing the bare soil spectral variations. The effect of this soil-induced vegetation noise was observed on continental scale NDVI imagery of Africa, where 'artifacts' seen in the Saharan desert were due to soil differences (Townshend and Justice, 1986; Huete and Tucker, 1991).
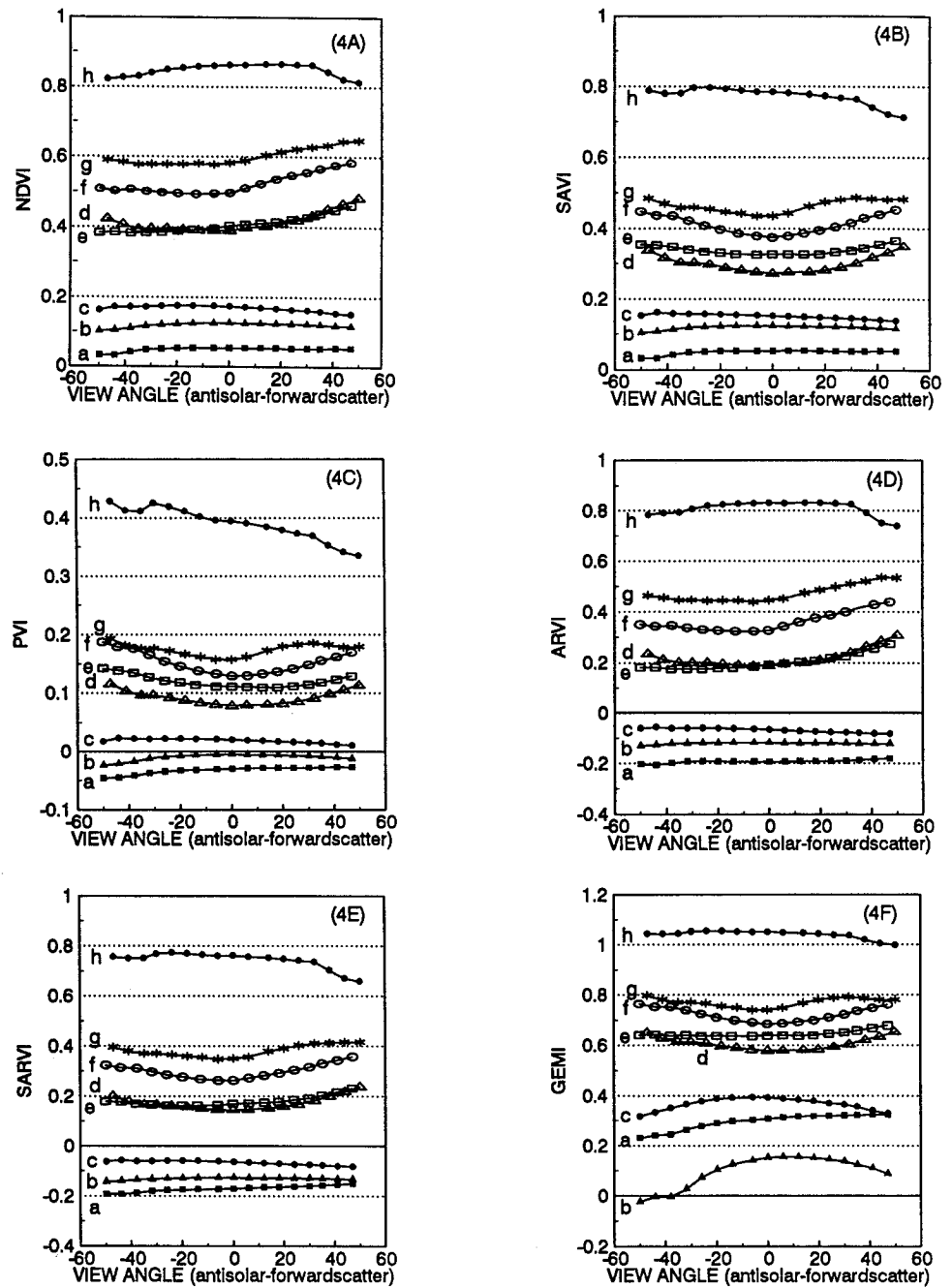
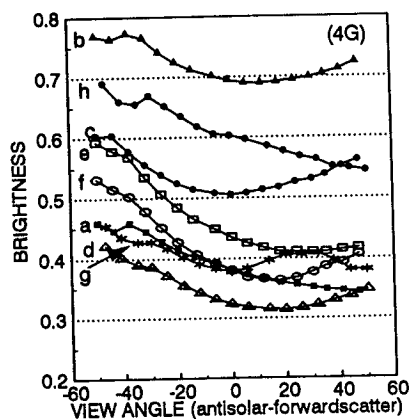Fig. 4. (see opposite page for caption)

Fig. 4. Response of vegetation indices to different vegetation covers and soils, and multiple view zenith angles. (A): NDVI; (B): SAVI; (C): PVI; (D): ARVI; (E): SARVI; (F): GEMI; (G): Brightness. Soils legend: a — laterite gravel and sand (■); b — bright sand (▲); c — bright sand and 20% litter (●). Vegetation legend: d — grass 20% (□); e — forb/grass 40% (△); f — grass 50% (○); g — grass 80% (∗); h — *Cassia* 100% (●). (DOY 213, 226 and 233; solar zenith ≈ 40°.)

3.4. The effect of sensor and sun geometry on VIs

The effect of view zenith angle on selected vegetation indices are shown in Figs. 4(A)–4(F) for different VIs, green vegetation covers and soils. The grass cover targets had a relatively dark soil background owing to organic matter deposits, compared with the forb/grass and the *Cassia* target. The vegetation in the last two targets also appeared more green and vigorous. The main phenologic difference between the grass and the *Cassia* vegetation cover was the stage of seedforming. Grasses had their inflorescences on top, which were less green than the leaves. *Cassia* was in a vigorous growing stage and was just starting to develop some small yellow flowers. A somewhat complex view angle response was seen depending upon the VI used, and the
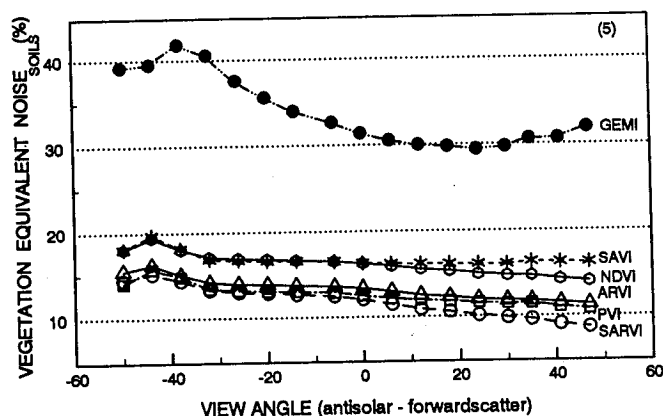

Fig. 5. Percentage vegetation equivalent noise (VEN$_{soils}$) induced by a range of bare soils as function of view zenith angle for selected vegetation indices (DOY 213, solar zenith 40°).

canopy structure and density. The resulting view angle profiles along the principal plane were concave for all partially vegetated canopies and convex to flat about nadir for *Cassia* and soils. Overall, it would appear that target anisotropy was greatest for sparse or incomplete grass canopies, and lowest for bare soil and dense canopies. In contrast to most of the grass vegetation sites, the grass/forb mixture (40% cover) was planophile and had a slightly flatter response than the erectophile grass covers.

The asymmetric response of NDVI, ARVI and SARVI with view angle (Fig. 4) appeared complex and difficult to model. The SAVI, PVI and GEMI, on the other hand, demonstrated a lack of dependency along the principal plane with a more symmetric response about nadir. Although empirical, Huete et al. (1992) normalized such view angle responses over a semi-arid grassland with a cosine function. This only works in partially vegetated canopies where the proportions of soil and plant were expected to change with viewing angle. The sunlit and shaded soil surfaces were further normalized by brightness-independent VIs, such as the SAVI. The brightness index (Fig. 4(G)) showed this strong anisotropic response about nadir attributed to the sunlit and shaded, soil and plant surfaces.

The solar principal plane is not necessarily the plane in which the satellite-based sensor systems view or scan the earth. For the location at Ouallam (Latitude 14.3°N and Longitude −1.95°E) the solar azimuth and solar principal plane is gradually increasing from the beginning of the growing season (DOY 175) to the peak of the growing season (DOY 250), while the satellite (AVHRR, Landsat, SPOT) scanning angle stays at 99° relative to North. In Table 5, solar azimuth and solar zenith angles are presented for SPOT, Landsat and AVHRR equatorial overpass times; 10:30 h GMT for SPOT, 09:45 h GMT for Landsat and 14:30 h GMT for AVHRR. These times are very close to the time of overpass at the Ouallam location. The difference of solar azimuth and the inclination angle at the time of overpass of the satellite sensor is about 30° in the beginning of the growing season, a few degrees during the peak green season and rapidly becomes greater again as vegetation is senescing.

In order to examine azimuthal effects, bidirectional reflectance measurements were

Table 5
Local (Quallam, Niger) solar azimuth and zenith angle for satellite overpass times

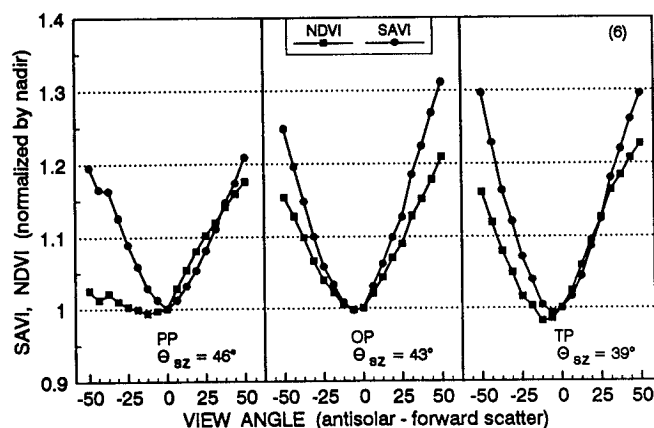| DOY	SPOT (10:30 h GMT, 98.7°)[a]		Landsat (09:45 h GMT, 98.2°)[a]		AVHRR (14:30 h GMT, 98.9°)[a]	
	Azimuth	Zenith	Azimuth	Zenith	Azimuth	Zenith
150	65.5	20.4	71.2	30.5	72.8	38.7
175	62.4	22.0	68.5	31.9	70.1	37.7
200	69.8	22.1	73.7	32.4	74.4	36.6
225	86.6	21.1	85.3	31.9	84.8	37.0
250	111.0	21.4	102.0	31.9	98.0	40.2
275	134.1	25.3	119.8	34.0	110.2	45.5
300	148.2	31.7	133.4	38.6	120.3	51.0

[a] Scanning angle of sensor; north is 0°.

Fig. 6. View azimuth angle and view zenith angle effects on SAVI and NDVI for medium (50%) grass cover. Annotations under the curves: PP — principal plane; OP — orthogonal plance; TP — tertiary plane; solar zenith angle (Θ_{sz}) at the time of the measurements (DOY 213).

made along three view azimuthal planes, the principal plane (82°), orthogonal plane (172°) and a third oblique plane (127°) to further examine view zenith and azimuth effects (Fig. 6). A non-symmetrical behavior was seen along the principal plane for the NDVI with a low and flat response in the backscatter direction and an increased response with forward scatter view angles. The SAVI had a more symmetrical response along all three measurement planes, and the NDVI also had a more symmetric response along both the orthogonal plane (OP) and the oblique plane (tertiary plane (TP), which was 45° to the PP). Although not shown in Fig. 6, the GEMI was symmetric for all azimuthal planes, while the PVI, ARVI and SARVI behaved irregular in the principal plane and more symmetric in the OP and TP. This means that it will be more difficult to correct the NDVI for the changing solar azimuth and view zenith angle effects, since a different correction must be applied for each stage of the growing season. The SAVI correction is mainly a function of view zenith angle only.

3.5. Diurnal changes of VIs owing to solar zenith angle and surface soil moisture

An understanding of solar zenith angle with sparse plant canopies is important since more or less soil may be illuminated. Depending on the view angle more or less of the illuminated or shaded soil may be viewed, which becomes important for geometric-optical modeling of VI response (Franklin et al., 1994). The diurnal (from morning to afternoon) NDVI responses based on nadir reflectances, for various targets are shown in Fig. 7. A strong solar zenith angle effect was observed in all canopies as all VIs decreased with smaller solar zenith angles.

A combined solar zenith and surface soil moisture effect on the NDVI was very pronounced in the sparse grass canopies (20 and 50% covers), as the wet soil surface in the morning darkened the soil surface and resulted in an NDVI that was nearly 20% higher than the afternoon response (dry soil surface) for the same solar zenith angles. At around 30° solar zenith angle, the surface of the soil underneath the grass
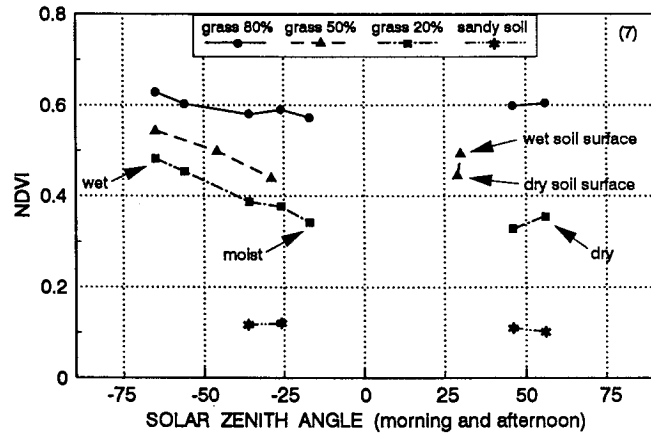
Fig. 7. NDVI response to solar zenith angle and soil moisture changes for different vegetation covers and nadir view angle (DOY 213 and 233).

cover becomes markedly drier and brighter. The 80% grass cover does show a solar zenith effect (Fig. 7), but not a soil moisture or any other effects (change in architecture, leaf turgidity, raindrops and dew on leaves), because morning (wet soil) and afternoon (dry soil) NDVI responses were similar for equal solar zenith angles.

To show the effect of surface soil moisture at a constant solar zenith angle, a controlled experiment was conducted: the spectral reflectance of a 50% green cover plot was measured dry and wet (water was sprinkled on the soil surface). Analogue to the VEN (vegetation equivalent noise) induced by different soils, the vegetation equivalent noise owing to surface soil moisture was formulated (Eq. (7)) to make a relative comparison between the selected VIs:

$$\%\mathrm{VEN_{wetness}} = 100(\mathrm{VI_{wet}} - \mathrm{VI_{dry}})_{target}/(\mathrm{VI_{full\,canopy}} - \mathrm{VI_{soils,mean}}) \qquad (7)$$

The 'surface soil moisture noise' was determined by $\mathrm{VI_{wet}} - \mathrm{VI_{dry}}$, which were the vegetation index responses of an identical vegetated target with wet and dry soil background, respectively. $\mathrm{VI_{soils,mean}}$ is the mean vegetation index response for bare soils and will be subtracted from $\mathrm{VI_{full\,canopy}}$ to account for the VI specific dynamic range. Figure 8 shows the percentage $\mathrm{VEN_{wetness}}$ for the selected VIs for the same target (50% green cover). A positive percent change meant a higher VI response with wetting and a negative percentage change was indicative of a lower VI response. Results for a 50% green cover were quantified in Table 4. The $\mathrm{VEN_{wetness}}$ owing to surface soil moisture increased the NDVI and the ARVI by about 7%, and the SARVI by 2%. The $\mathrm{VEN_{wetness}}$ for GEMI, PVI and GVI was about 2%, 1% and 2%, respectively. The surface soil moisture effect was best minimized with the SAVI (−0.3%). If the VI response to wetting were to be linear between 0 and 50% green cover, $\mathrm{VEN_{wetness}}$ would give the percentage change in VI for other partially vegetated targets as well.

N-space VIs have, beside a 'greenness' component (PVI and GVI), a 'brightness' component. Because 'brightness' is not a VI, the $\mathrm{VI_{soils,mean}}$ can be set to zero in Eq. (7) which then becomes a brightness based soil moisture indicator. Figure 8 shows the percentage change in brightness of the target owing to a wet soil background, relative
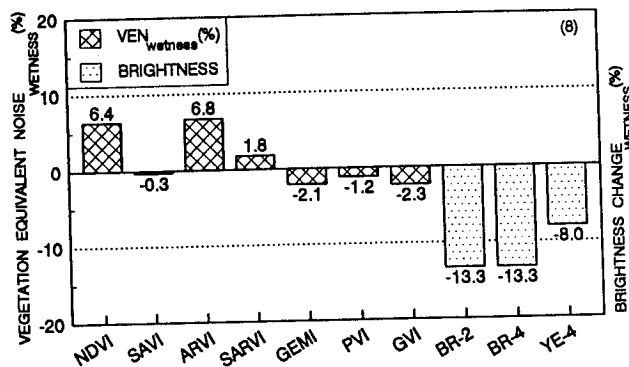
Fig. 8. Vegetation equivalent noise (VEN$_{wetness}$) induced by surface soil moisture for a 50% grass cover, using nadir VI responses. The brightness (BR-2-space and BR-4-space) and yellowness (YE-4-space) sensitivity to soil moisture is shown by the last three bars.

to a dry soil background of the same target. Brightness decreased by about 13% for this particular target. The yellowness component was not observed to yield extra information other than another brightness indicator.

3.6. Temporal vegetation dynamics

Bush/grassland transect radiometric data were collected at about 40° solar zenith angle, but slightly different soil surface moisture conditions (Table 1). Plant cover estimates and 10 biomass samples were taken along the same transects for which the data is presented. The radiometric data showed no significant difference between the two parallel transects in both the bush/grassland and the degraded bushland. Despite the grazing on parts of the transects, both cover estimates and VIs increased with time (Fig. 9). Biomass was doubled during the observation period (Table 1).

A method to look at vegetation dynamics for the growing season was to measure a range of representative vegetation covers and determine the relation between radiometric data products (VIs) and biophysical data. The transect averages then can be converted to cover and or biomass. The line in Fig. 9 presents the relationship between the BRF control plots from Fig. 4 (using nadir measurements) and estimated vegetation cover. As can be seen, the VI relationship with the transect vegetation cover was different from the relationship obtained with the BRF control plots. Some uncertainty is possibly introduced by the method of cover estimation (step transect) which might have overestimated the green cover. Furthermore, the control plots had less than 1% dead standing biomass or litter. Knowing that there was about 9% litter on the soil surface or as standing dead biomass, of which the majority was standing, the VI response was lowered owing to the standing dead biomass obscuring the green plants. On the other hand, one set of points involved temporal variations (transects), while the other set involved spatial differences (control plots) which include a wide variety of cover types. Thus, the SAVI and NDVI may be fair indicators of temporal changes in vegetation cover, but may be less effective in detecting spatial differences in cover, since there was a non-linear relation
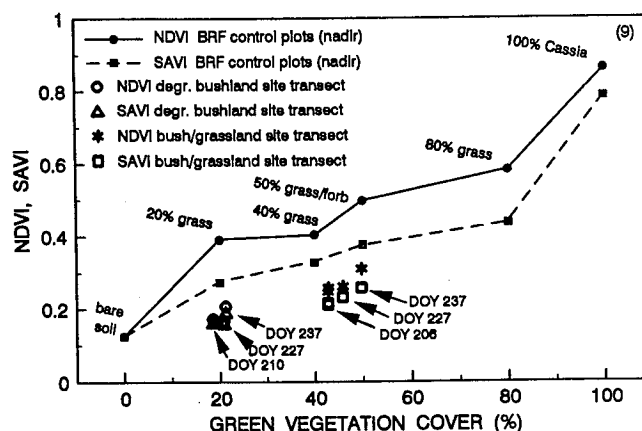
Fig. 9. Relationship between green cover, and the SAVI and NDVI for BRF control plots and the temporal average transect responses of the grass/bushland site and the degraded bushland site.

between the VIs and the vegetation covers at the bush/grassland and degraded bushland, and the grass and *Cassia* control plots.

It was also noticeable that the VIs were responding more to a vigorous green looking *Cassia* canopy (100% cover) than to a light green 80% partial grass cover (Fig. 9). The grass control plots were observed to have very different phenologic stages in comparison with the *Cassia*, which was starting to flower. Not only were the grasses flowering and in a fruiting stage, the leaf angle distribution was erectophile and not planophile as with the *Cassia* canopy. Furthermore, *Cassia* (100% green cover) had lower green biomass than the grass (80% green cover) (Table 1). One could conclude that the VIs were not consistent at a single site for a single vegetation cover.

4. Concluding remarks

The spectral signatures of different soils, vegetation species and landscapes showed significant variability. It was obvious that the BRF of the different soil and vegetation types were a function of sun and view geometry. Both soil and vegetation types had anisotropic reflectance properties. The results of the optical characterization of the Sahelian grass savannah presented here were similar to the results for the semi-desert grassland in Arizona (Huete et al., 1992).

The effect of solar zenith angle on nadir reflectances and corresponding VIs was significant and should be taken into account in any normalization process if comparisons are to be made among biomes on a global scale. Similar results were found in a study by Middleton (1991), who looked at the effect of solar zenith angle on the NDVI for the tallgrass prairie in Kansas. The solar azimuth angle was important for global and regional scale VI products, because azimuth angle changed largely with respect to satellite sensor inclination angle at higher latitudes. NDVI, ARVI and SARVI behaved asymmetrically about nadir for off-nadir view angles, while SAVI had the best symmetric response to view angle.

The SAVI, GEMI and n-space vegetation indices (PVI and GVI) did discriminate between 20 and 40% green vegetation cover targets. The NDVI, ARVI and SARVI did not separate 20% from the 40% vegetation cover. The PVI and GVI lacked dynamic range, but the brightness index provided some extra useful information, particularly related to surface moisture and other soil related influences.

Soil background influences were shown to alter the response of VIs. SARVI looked promising for discriminating low vegetation covers from soil (Fig. 5) and had the best capabilities for detecting low levels of green vegetation. The GEMI showed a large dynamic range for different soils, which was not a good quality in a VI.

NDVI and ARVI were altered seriously by surface soil moisture effects, while the SAVI had the least sensitivity to soil moisture in vegetated canopies as shown in Fig. 8 by the VEN$_{wetness}$. Soil brightness (n-space) was an indication of soil surface wetness when a temporal profile for the same area was monitored. This was observed for a temporal profile of NDVI, SAVI and n-space 'brightness' for bush/grassland. Especially with the bright sandy soils, a large difference was observed between a dry and a wet (dark) soil background. Soil brightness could also be helpful to make a VI soil baseline correction for a specific landscape unit, since the VI response of bare soil seems to be related to brightness. Escadafal and Huete (1991) used a redness index to adjust VIs for 'soil noise' with promising results.

The inclusion of the blue band in the ARVI and SARVI did not show a significant aggravation of soil background effects. The ARVI and SARVI behaved similarly as the NDVI and SAVI, respectively. The SARVI therefore has strong potential if the utilized blue, red and NIR wavebands can be corrected for Rayleigh and ozone atmosphere effects, and the NIR waveband is not affected by atmospheric water vapor. If atmospheric corrections of satellite data cannot be made, the self correcting GEMI might become more useful, although it was showed to be not very applicable for sparsely vegetated areas and with atmosphere free, ground data.

All VIs had a non-linear relationship with the different vegetation covers. SAVI and NDVI seemed fair indicators of the temporal vegetation changes, but did not respond well to the spatial differences involving different vegetation species and soils.

Overall there was no 'optimal' VI, however, the SAVI, SARVI and PVI seemed to perform best under most of the adverse conditions (vegetation cover, soil color/brightness, soil moisture, and sun and view geometry) and should be used in estimating vegetation growth in the Sahelian zone.

Acknowledgments

References

Baret, F. and Guyot, G., 1991. Potentials and limits of vegetation indices for LAI and APAR assessment. Remote Sens. Envrion., 35: 161–173.

Bégué, A., Hanan, N. and Prince, S.D., 1994. Radiative transfer in shrub savanna sites in Niger: preliminary results from HAPEX-Sahel. 2. Photosynthetically active radiation interception of the woody layer. Agric. For. Meteorol., 69: 247–266.

Bonham, C.D., 1989. Measurements for Terrestrial Vegetation. John Wiley, New York, 338 pp.

Colwell, J.E., 1974. Vegetation Canopy Reflectance. Remote Sens. Envrion., 3: 175–183.

Escadafal, R. and Huete, A.R., 1991. Improvement in remote sensing of low begetation cover in arid regions by correcting vegetation indices for soil "noise". Pedology. C.R. acad. Sci. Paris, t. 312, Serie II, pp. 1385–1391.

Franklin, J., Duncan, J., Huete, A.R., van Leeuwen, W.J.D., Li, X. and Bégué, A., 1994. Radiative transfer in shrub savanna sites in Niger: preliminary results from HAPEX-Sahel. 1. Modelling surface reflectance using a geometric-optical approach. Agri. For. Meteorol., 69: 223–245.

Goutorbe, J.-P., Lebel, T., Tinga, A., Bessemoulin, P., Brower, J. et al., 1994. HAPEX-Sahel: a large scale study of land-atmosphere interactions in the semi-arid tropics. Ann. Geophys. (submitted).

Huete, A.R., 1988. A soil adjusted vegetation index (SAVI). Remote Sens. Envrion., 25: 295–309.

Huete, A.R. and Tucker, C.J., 1991. Investigation of soil influences in AVHRR red and near-infrared vegetation index imagery. Int. J. Remote Sensing, 12: 1223–1242.

Huete, A.R., Post, D.F. and Jackson, R.D., 1984. Soil spectral effect on 4-space vegetation discrimination. Remote Sens. Environ., 15: 155–165.

Huete, A.R., Hua, G., Qi, J., Chehbouni, A. and van Leeuwen, W.J.D., 1992. Normalization of multi-directional red and NIR reflectances with the SAVI. Remote Sens. Envrion., 40: 1–20

Jackson, R.D., 1983. Spectral indices in n-space. Remote Sens. Environ., 13: 409–421

Jackson, R.D., Moran, M.S., Gay, L.W. and Raymond, L.H., 1987. Evaluating evaporation from field crops using airborne radiometry and ground-based meteorological data. Irrig. Sci., 8: 81–90.

Jackson, R.D., Teillet, P.M., Slater, P.N., Fedosejevs, G., Jasinski, M.F. et al., 1990. Bidirectional measurements of surface reflectance for view angle corrections of oblique imagery. Remote Sens. Environ., 32: 189–202.

Justice, C.O. and Hiernaux, P.H.Y., 1986. Monitoring the grasslands of the Sahel using NOAA/AVHRR data: Niger 1983. Int. J. Remote Sens., 30: 261–270.

Justice, C.O., Dugdale, G., Townshend, J.R.G., Narracott, A.S. and Kumar, M., 1991. Synergysm between NOAA-AVHRR and Meteosat data for studying vegtation development semi-arid West Africa. Int. J. Remote Sensing, 12: 1349–1368.

Kaufman, Y.J., and Tanre, D., 1992. Atmospherically resistant vegetation index (ARVI) for EOS-MODIS. IEEE Trans. Geosci. Remote Sens., 30: 261–270.

Kauth, R.J. and Thomas, G.S., 1976. The Tasseled Cap — a graphic description of spectral-temporal development of agricultrual crops as seen by Landsat. Proc. Symp. on Machine Processing of Remotely Sensed Data, Perdue University, West Lafayette, IN, pp. 41–51.

Middleton, E.M., 1991. Solar zenith angle effects on vegetation indices in tallgrass prairie. Remote Sens. Envrion., 38: 45–62.

Moran, M.S., Jackson, R.D., Raymond, L.H., Gay, L.W. and Slater, P.N., 1989. Mapping surface energy balance components by combining Landsat thematic mapper and ground-based meteorologic data. Remote Sens. Envrion., 30: 77–87.

Payne, W.A., Wendt, C.W. and Lascano, R.J., 1990. Bare fallowing on sandy fields in Niger, West Africa. Soil Sci. Soc. Am. J., 54(4), 1079–1084.

Pinty, B. and Verstraete, M.M., 1992. GEMI: A non-linear index to monitor vegetation from satellites. Vegetatio, 101: 15–20.

Richardson, A.J. and Wiegand, C.L., 1977. Distinguishing vegetation from soil background information. Photogramm. Eng. Remote Sens., 43: 1541–1552.

Townshend, J.R.G. and Justice, C.O., 1986. Analysis of the dynamics of African vegetation using the normalized difference vegetation index. Int. J. Remote Sens., 7: 1435–1445.

Wylie, B.K., Harrington, Jr., J.A., Prince, S.D. and Denda, I., 1991. Satellite and ground-based pasture production assessment in Niger: 1986–1988. Int. J. Remore Sens., 12: 1281–1300.

GENERAL INFORMATION

A detailed *Guide for Authors* is available upon request, and will also be printed in the first issue to appear in each year's subscription. You are kindly asked to consult this guide. Please pay special attention to the following notes.

Language

The official language of the journal is English, but occasional articles in French and German will be considered for publication. Such articles should start with an abstract in English, headed by an English translation of the title. An abstract in the language of the paper should follow the English abstract. English translations of the figure captions should also be given.

Preparation of the text

a) The manuscript should be typewritten with double spacing and wide margins and include at the beginning of the paper an abstract of not more than 500 words. Words to be printed in italics should be underlined. The metric system should be used throughout.

b) The title page should include: the title, the name(s) of the author(s) and their affiliations.

References

a) References in the text start with the name(s) of the author(s), followed by the publication date in parentheses.

b) The reference list should be in alphabetical order and on sheets separate from the text.

Tables

Tables should be compiled on separate sheets. A title should be provided for each table and they should be referred to in the text.

Illustrations

a) All illustrations should be numbered consecutively and referred to in the text.

b) Drawings should be completely lettered, the size of the lettering being appropriate to that of the drawings, but taking into account the possible need for reduction in size (preferably not more than 50%). The page format of *Agricultural and Forest Meteorology* should be considered in designing the drawings.

c) Photographs must be of good quality, printed on glossy paper.

d) Figure captions should be supplied on a separate sheet.

Proofs

One set of proofs will be sent to the author, to be checked for printer's errors. In the case of two or more authors please indicate to whom the proofs should be sent.

Submission of manuscripts

For North America: Dr. Kyaw T. Paw U, LAWR, Atmospheric Sciences, Hoagland Hall, University of California, Davis, CA 95616, USA

For Europe, Africa and the Middle East: Dr. James R. Milford, Department of Meteorology, University of Reading, 2, Earley Gate, Reading RG6 2AU, UK

For Asia, Australia, New Zealand, Central and South America: Dr. Ray Leuning, Centre for Environmental Mechanics, G.P.O. Box 821, Canberra, A.C.T. 2601, Australia

A manuscript rejected for publication in *Agricultural and Forest Meteorology* may not be resubmitted.

Manuscript and illustrations should be submitted in triplicate. One set should be in a form ready for reproduction: the other two may be of lower quality. Submission of an article is understood to imply that the article is original and unpublished and is not being considered for publication elsewhere. Upon acceptance of an article by the journal, the author(s) will be asked to transfer the copyright of the article to the publishers. This transfer will ensure the widest possible dissemination of information.

Submission of electronic text

In order to publish the paper as quickly as possible after acceptance, authors are encouraged to submit the final text also on a 3.5″ or 5.25″ diskette. Both double density (DD) and high density (HD) diskettes are acceptable. Make sure, however, that the diskettes are formatted according to their capacity (HD or DD) before copying the files onto them. Similar to the requirements for manuscript submission, main text, list of references, tables and figure legends should be stored in separate text files with clearly identifiable file names. The format of these files depends on the word processor used. Texts made with DisplayWrite, MultiMate, Microsoft Word, Samna Word, Sprint, Volkswriter, Wang PC, WordMARC, WordPerfect, Wordstar, or supplied in DCA/RFT, or DEC/DX format can be readily processed. In all other cases the preferred format is DOS text or ASCII. It is essential that the name and version of the wordprocessing program, type of computer on which the text was prepared, and format of the text files are clearly indicated. Authors are encouraged to ensure that **the disk version and the hardcopy must be identical**. Discrepancies can lead to proofs of the wrong version being made.